Room-Temperature Phosphorescence Sensor Array for Detection and Discrimination of Neonicotinoid Insecticides based on Host-Guest Doping

Caicai Liu, [a, b] Ran Li, [b] Peng Yun, [c] Fuzun Chen, [c] Yu-e Shi, [a, b] Xiaobo Zhu, [c,*] Zhenguang Wang [a, b*]

[a] Key Laboratory of Medicinal Chemistry and Molecular Diagnosis, Ministry of Education, College of Chemistry & Materials Science, Hebei University, Baoding 071002, P. R. China
[b] Hebei Key Laboratory of Inorganic Nanomaterials, Hebei Technology Innovation Center for Energy Conversion Materials and Devices, College of Chemistry and Material Science, Hebei Normal University, Shijiazhuang, Hebei, 050024, China; Email: zgwang@hbu.edu.cn.

[c] Hebei Province Center for Disease Prevention and Control, Shijiazhuang 050021, China

Figures

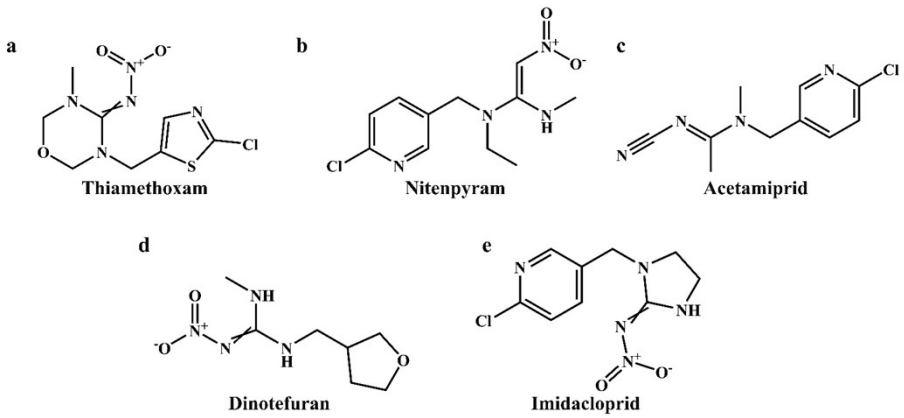

Figure S1. Chemical structures of five types of NNI.

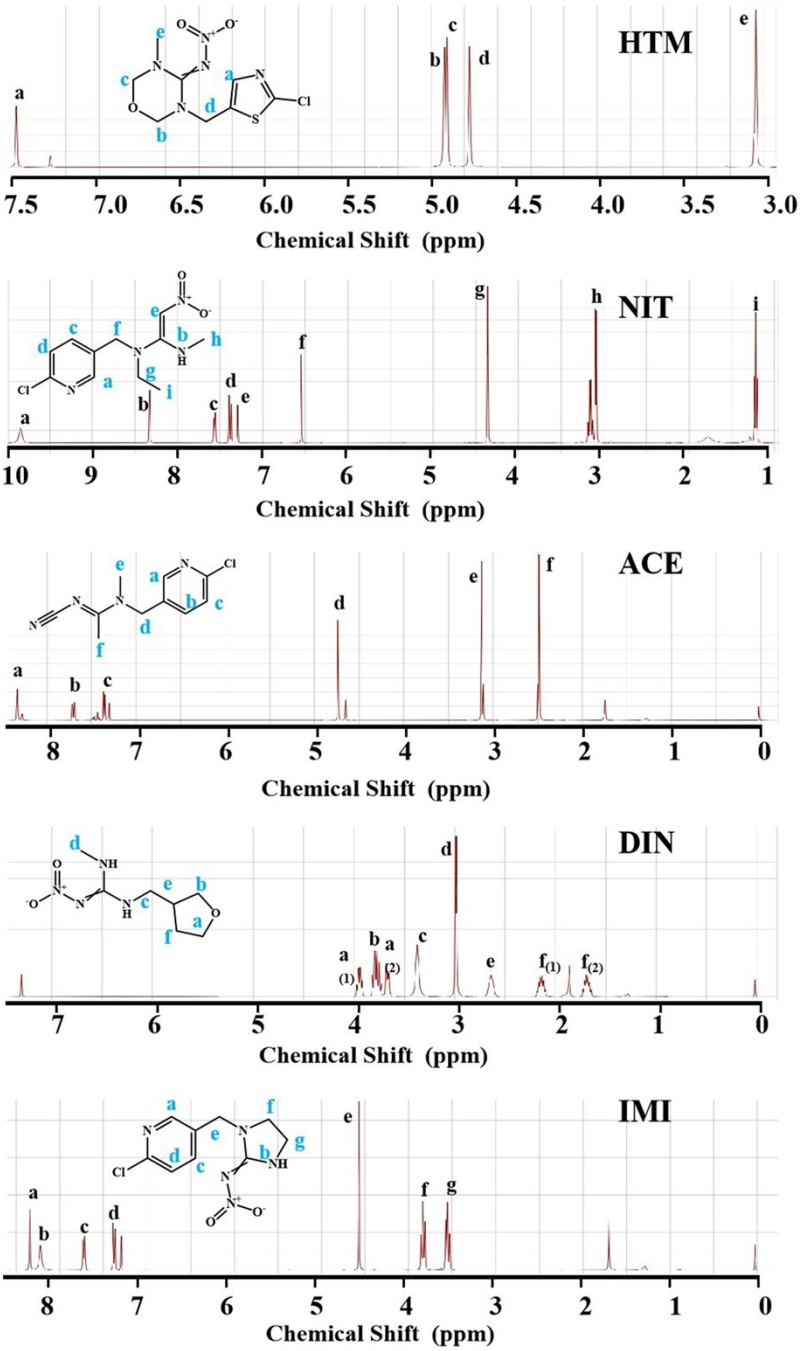

Figure S2. ^{1}H NMR spectra of different types of NNI.

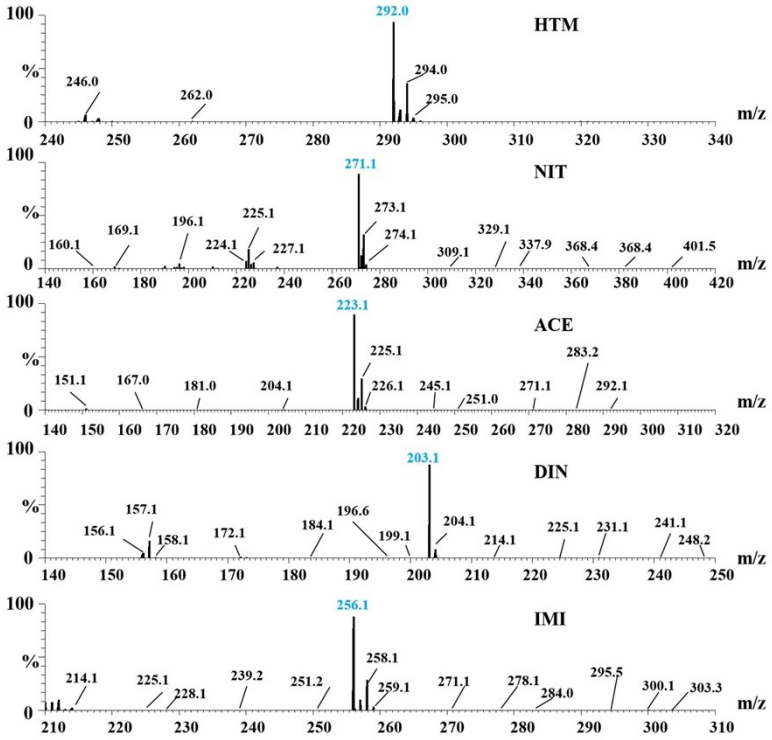

Figure S3. High-resolution mass spectra of different types of NNI.

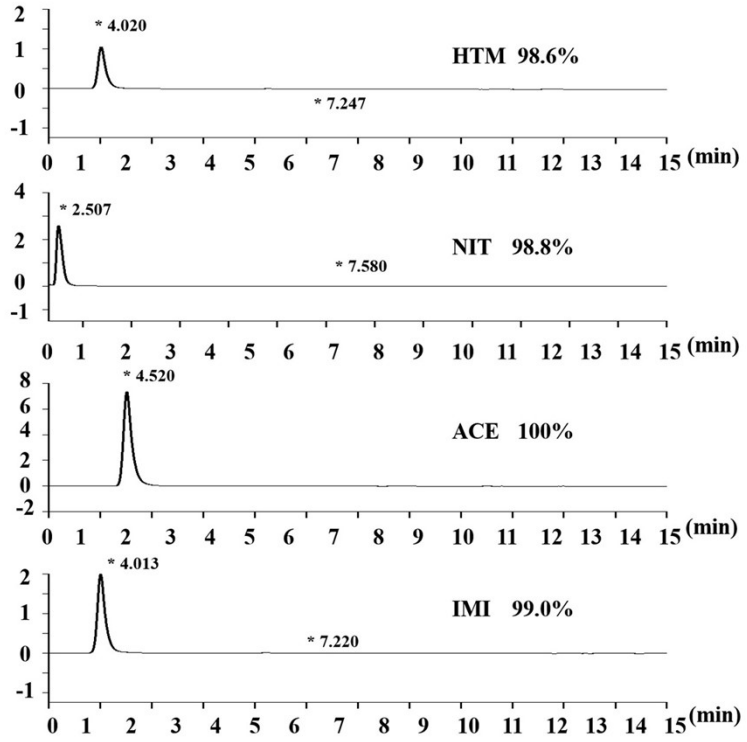

Figure S4. HPLC results of different types of NNI.

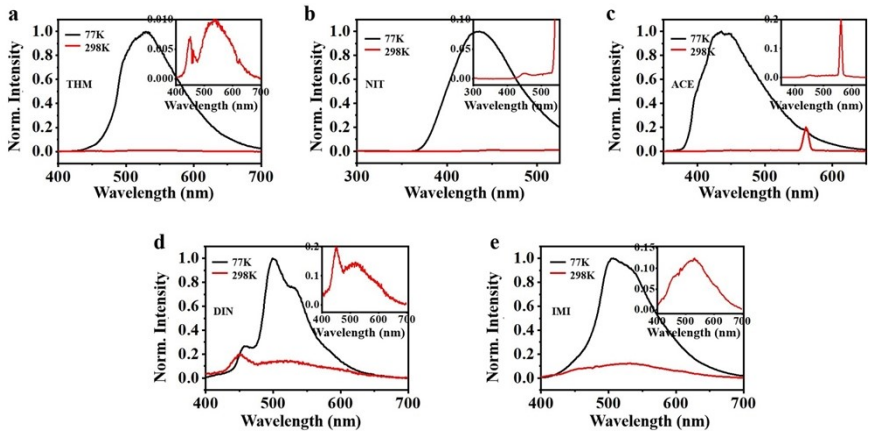

Figure S5. Delayed PL spectra of five types of NNI recorded at 298 K (red line) and 77 K (black line).

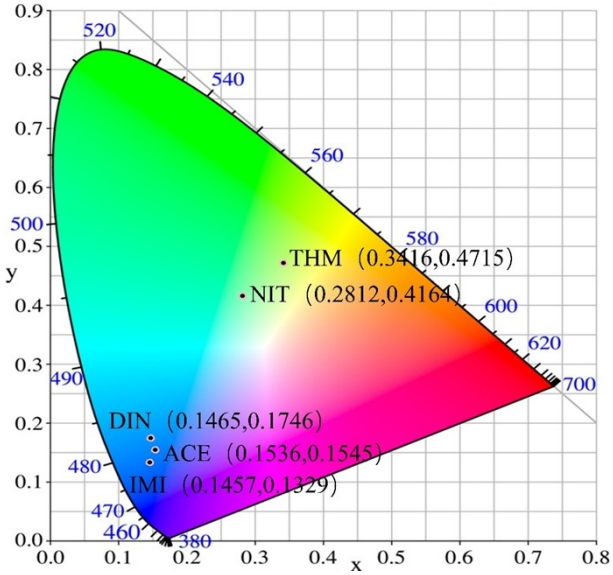

Figure S6. CIE color coordinates of five types of afterglow materials produced by doping different types of NNI.

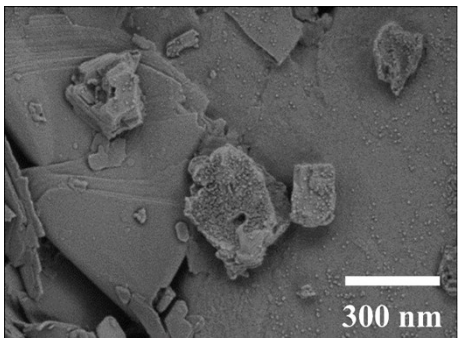

Figure S7. SEM image of BA@NNI.

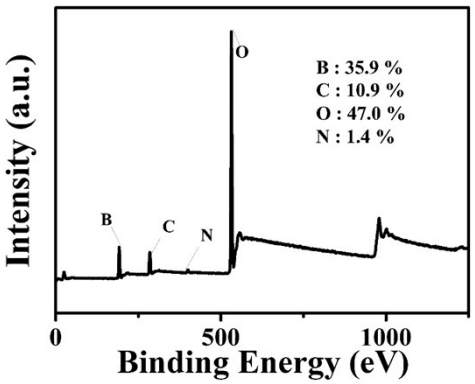

Figure S8. Full scan XPS spectrum of BA@NNI.

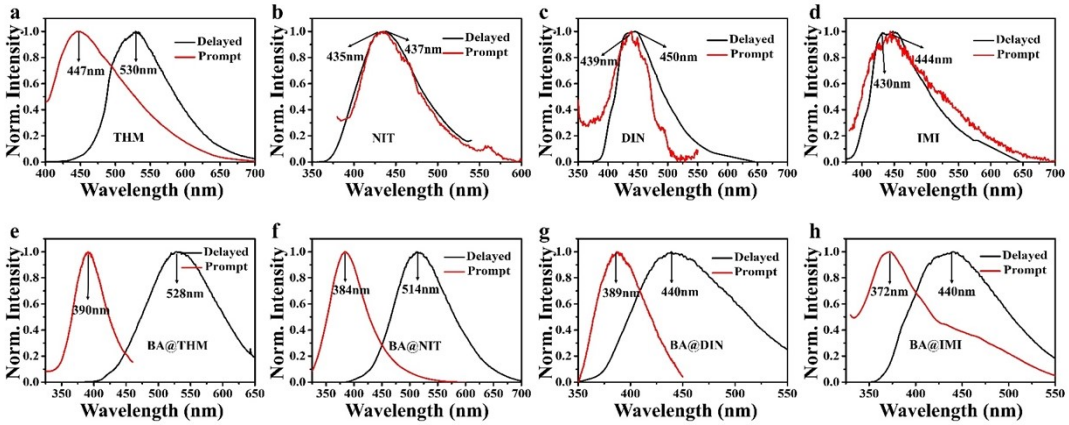

Figure S9. Prompt PL spectra at 298 K (red line) and the delayed PL spectra at 77 K (black line) of five types of BA@NNI.

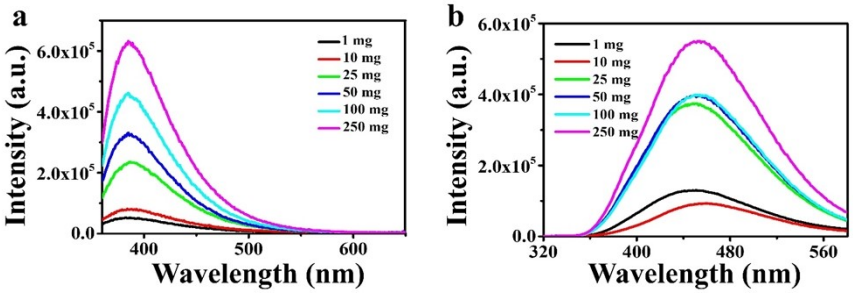

Figure S10. Prompt (a) and delayed PL (b) spectra of BA@NNI, producing by loading different amount of NNI.

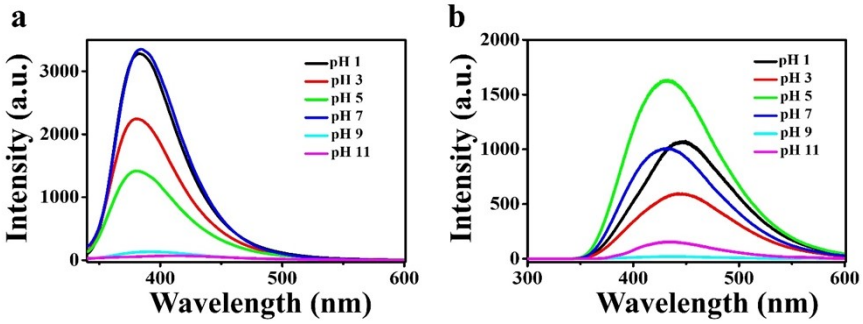

Figure S11. Prompt (a) and delayed PL (b) spectra of BA@NNI, producing by reacting at different pH values.

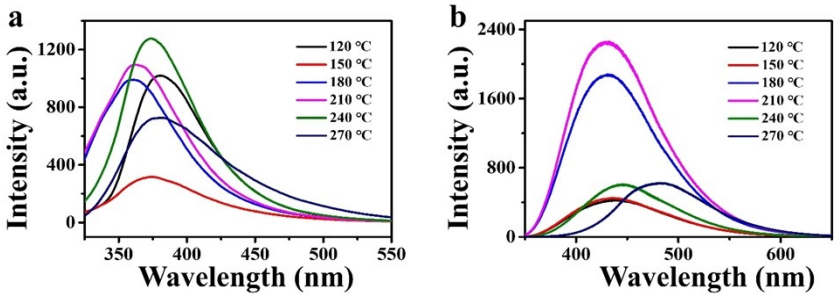

Figure S12. Prompt (a) and delayed PL (b) spectra of BA@NNI, producing by reacting at different temperatures.

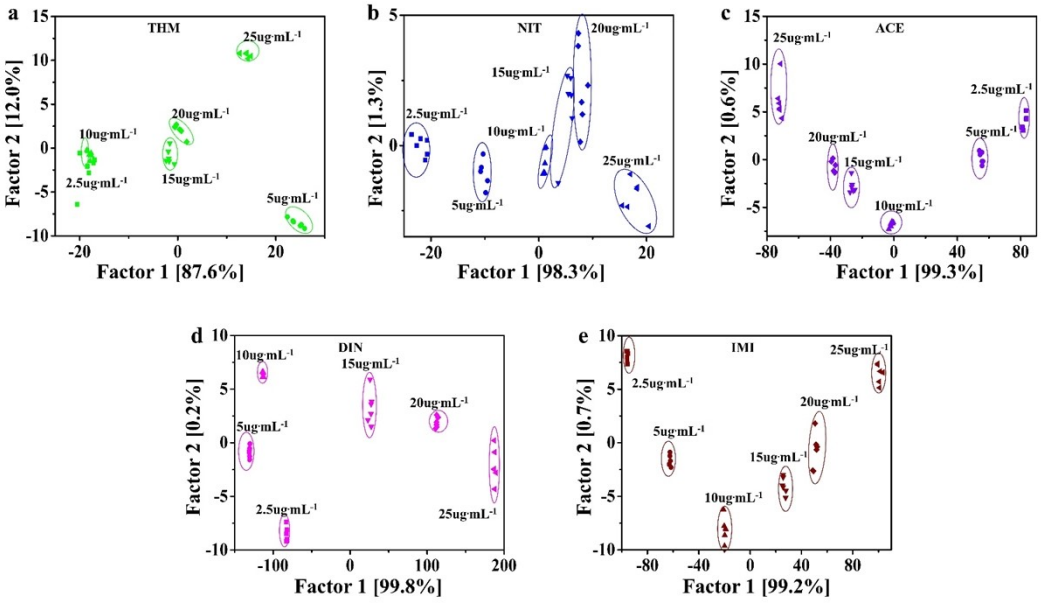

Figure S13. PCA dendrogram for the assay against different concentration of NNI.

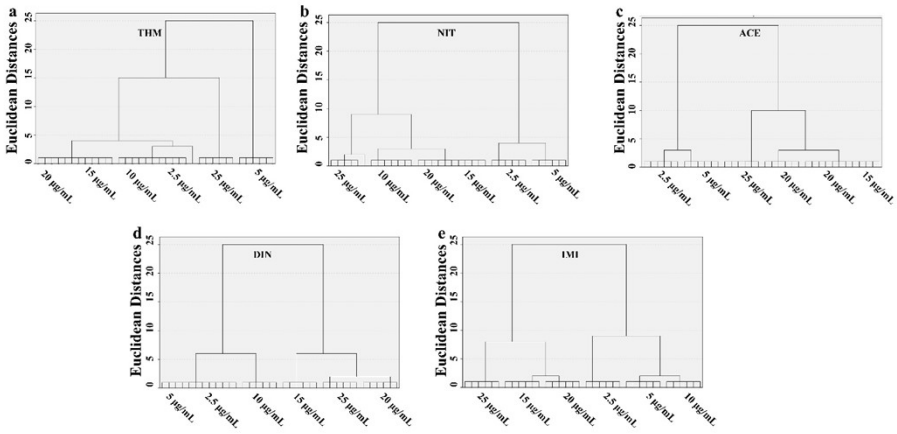

Figure S14. HCA dendrogram for the assay against different concentration of NNI.

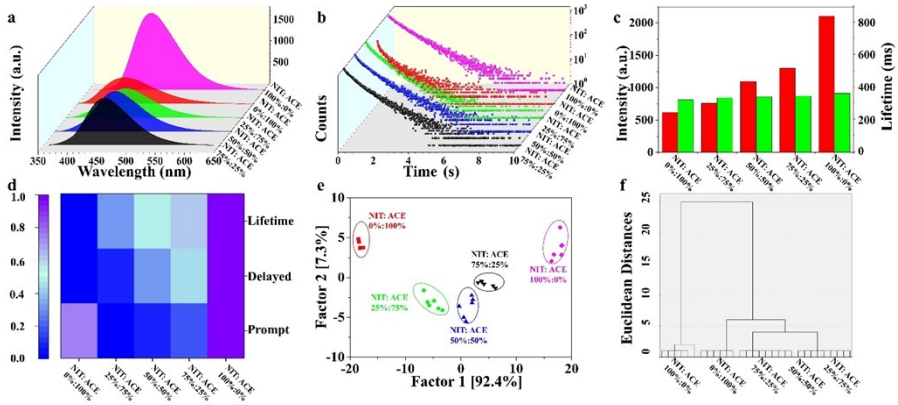

Figure S15. Delayed PL spectra (a), emission decay curves (b), and the PL intensity and average emission lifetime (c) of RTP materials after loading different mixtures; (d) heat map, LDA plot (e) and HCA dendrogram (f) for the discriminating the mixtures.

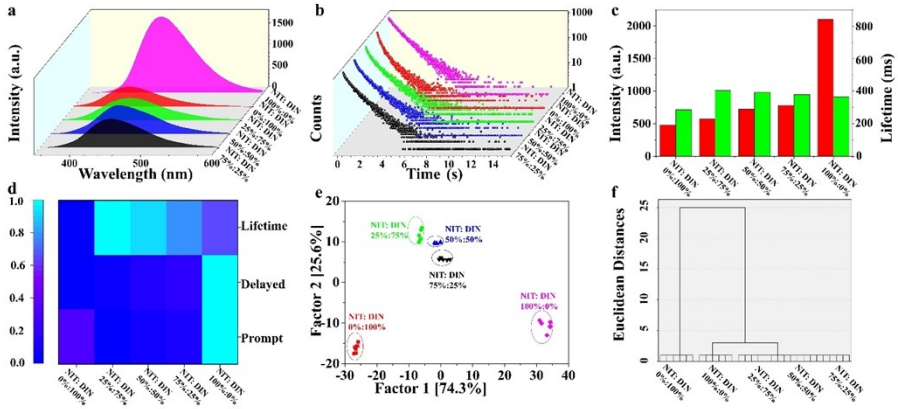

Figure S16. Delayed PL spectra (a), emission decay curves (b), and the PL intensity and average emission lifetime (c) of RTP materials after loading different mixtures; (d) heat map, LDA plot (e) and HCA dendrogram (f) for the discriminating the mixtures.

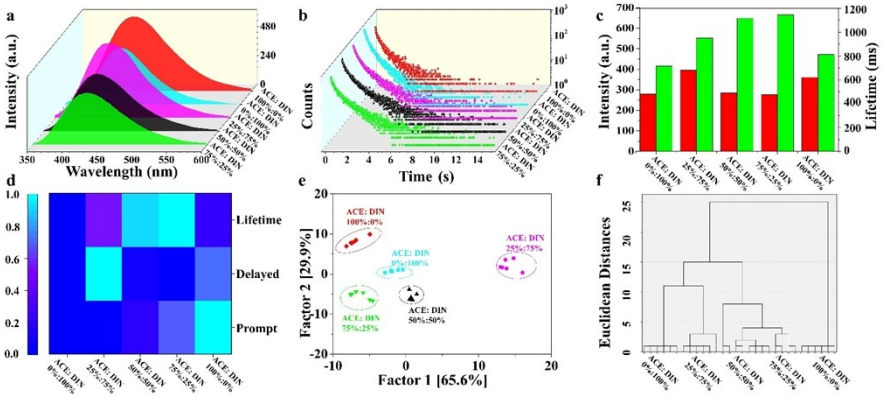

Figure S17. Delayed PL spectra (a), emission decay curves (b), and the PL intensity and average emission lifetime (c) of RTP materials after loading different mixtures; (d) heat map, LDA plot (e) and HCA dendrogram (f) for the discriminating the mixtures.

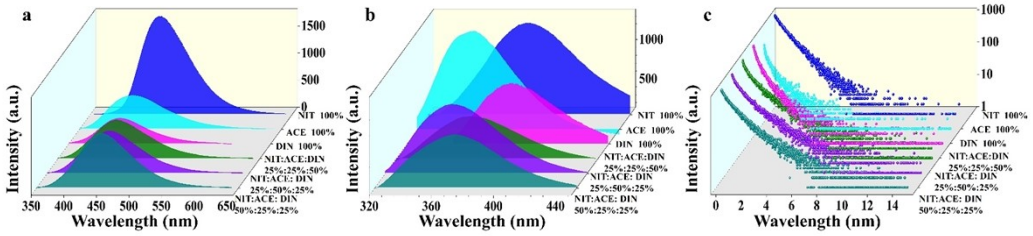

Figure S18. Prompt (a), delayed PL spectra (b), emission decay curves (c) of RTP materials after loading different mixtures.

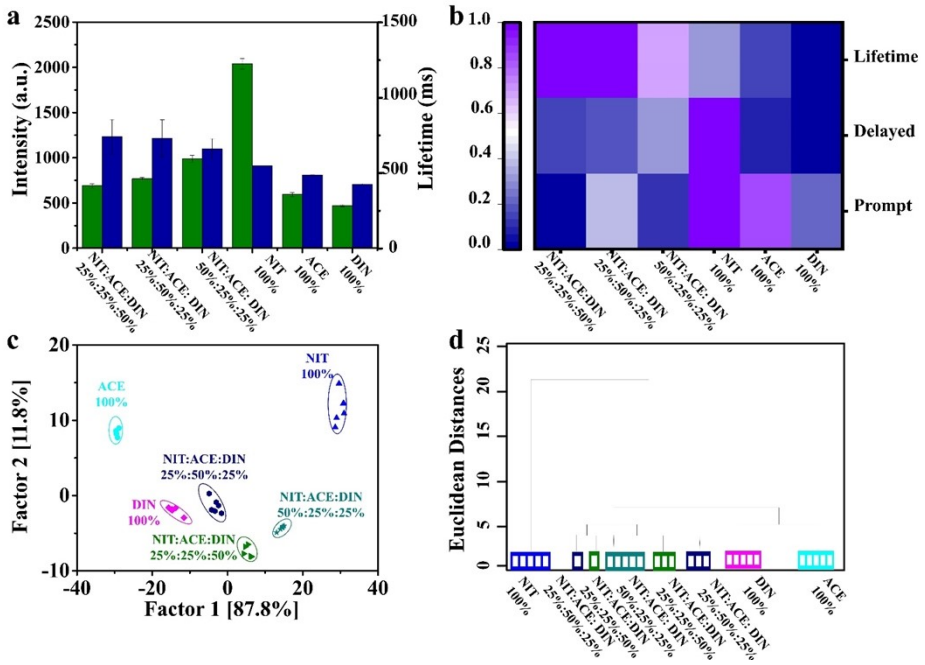

Figure S19. (a) The delayed PL, prompt PL intensities, and emission lifetime of ternary mixtures;

(b) Heat map obtained from delayed PL, prompt PL intensity and emission lifetimes for different types of mixtures; LDA plot (c) and HCA dendrogram (d) for the discriminating the ternary mixtures.

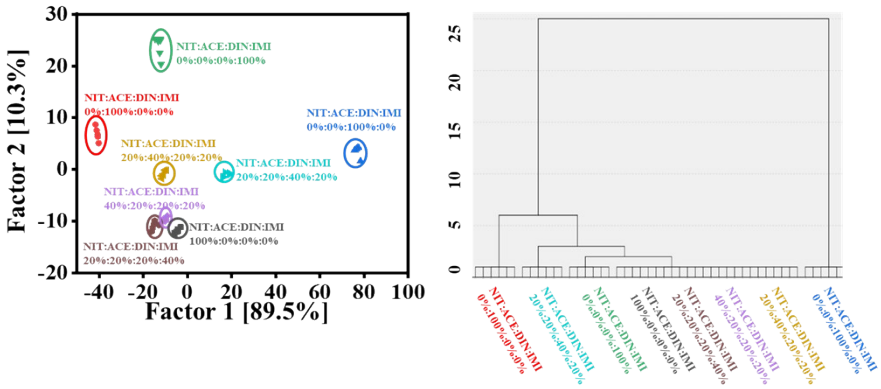

Figure S20. LDA plot (left) and HCA dendrogram (right) for the discriminating the quadratic mixtures.

Tables

Table S1. The energy levels of singlet and triplet excited states and SOC constant of THM.

Molecule	Transition	E_{S1}-E_{Tn} (eV)	SOC (cm^{-1})
THM	$S_1 \rightarrow T_1$	0.91	0.48
	$S_1 \rightarrow T_2$	0.46	38.81
	$S_1 \rightarrow T_3$	-1.44	40.90
	$S_1 \rightarrow T_4$	-1.48	22.19
	$S_1 \rightarrow T_5$	-1.61	20.92
	$S_1 \rightarrow T_6$	-2.49	0.81
	$S_1 \rightarrow T_7$	-2.92	3.18
	$S_1 \rightarrow T_8$	-2.99	1.87
	$S_1 \rightarrow T_9$	-3.07	2.83
	$S_1 \rightarrow T_{10}$	-3.19	14.65

Table S2. The energy levels of singlet and triplet excited states and SOC constant of NIT.

Molecule	Transition	E_{S1}-E_{Tn} (eV)	SOC (cm^{-1})
NIT	$S_1 \rightarrow T_1$	0.50	20.35
	$S_1 \rightarrow T_2$	0.31	42.47
	$S_1 \rightarrow T_3$	-0.21	0.13
	$S_1 \rightarrow T_4$	-1.12	13.59
	$S_1 \rightarrow T_5$	-1.43	0.82
	$S_1 \rightarrow T_6$	-1.62	29.11
	$S_1 \rightarrow T_7$	-1.94	2.24

	$S_1 \rightarrow T_8$	-1.99	0.36
	$S_1 \rightarrow T_9$	-2.26	13.44
	$S_1 \rightarrow T_{10}$	-2.84	6.48

Table S3. The energy levels of singlet and triplet excited states and SOC constant of ACE.

Molecule	Transition	E_{S1}-E_{Tn} (eV)	SOC (cm^{-1})
ACE	$S_1 \rightarrow T_1$	0.79	5.55
	$S_1 \rightarrow T_2$	0.31	0.26
	$S_1 \rightarrow T_3$	-0.07	14.78
	$S_1 \rightarrow T_4$	-0.54	4.55
	$S_1 \rightarrow T_5$	-0.72	8.86
	$S_1 \rightarrow T_6$	-0.99	0.62
	$S_1 \rightarrow T_7$	-1.19	1.31
	$S_1 \rightarrow T_8$	-1.76	2.66
	$S_1 \rightarrow T_9$	-1.79	0.26
	$S_1 \rightarrow T_{10}$	-2.23	5.06

Table S4. The energy levels of singlet and triplet excited states and SOC constant of DIN.

Molecule	Transition	E_{S1}-E_{Tn} (eV)	SOC (cm^{-1})
DIN	$S_1 \rightarrow T_1$	0.93	51.32
	$S_1 \rightarrow T_2$	0.46	15.36
	$S_1 \rightarrow T_3$	-1.46	24.37
	$S_1 \rightarrow T_4$	-1.74	18.73
	$S_1 \rightarrow T_5$	-2.55	9.40

	$S_1 \rightarrow T_6$	-3.10	11.93
	$S_1 \rightarrow T_7$	-3.29	7.70
	$S_1 \rightarrow T_8$	-4.31	3.09
	$S_1 \rightarrow T_9$	-4.46	7.59
	$S_1 \rightarrow T_{10}$	-4.51	4.77

Table S5. The energy levels of singlet and triplet excited states and SOC constant of IMI.

Molecule	Transition	E_{S1}-E_{Tn} (eV)	SOC (cm^{-1})
IMI	$S_1 \rightarrow T_1$	0.78	51.91
	$S_1 \rightarrow T_2$	0.46	0.50
	$S_1 \rightarrow T_3$	-1.18	4.38
	$S_1 \rightarrow T_4$	-1.55	1.23
	$S_1 \rightarrow T_5$	-1.60	25.14
	$S_1 \rightarrow T_6$	-2.13	1.98
	$S_1 \rightarrow T_7$	-2.35	24.17
	$S_1 \rightarrow T_8$	-2.39	0.42
	$S_1 \rightarrow T_9$	-2.66	7.48
	$S_1 \rightarrow T_{10}$	-2.83	0.54

Table S6. Delayed and prompt PL emission lifetimes ($\tau_{1\text{-}2,\ ms/ns}$) and fractions of the emission intensity ($f_{1\text{-}2}$, %) obtained from the fitting of experimental emission decay data by two-exponential functions of different materials, from which the average emission lifetimes τ_{avg} were calculated.

Sample	Delayed			Prompt		
	τ_1 (f_1)	τ_2 (f_1)	$\tau_{avg\ (ms)}$	τ_1 (f_1)	τ_1 (f_1)	$\tau_{avg\ (s)}$
BA@THM	386.04(30.0)	1577.00(70.0)	1220	0.79(50.0)	4.15(50.0)	2.47
BA@NIT	418.39(28.5)	1194.60(71.2)	973	2.08(47.7)	7.92(52.3)	5.14
BA@ACE	374.06(31.9)	1466.81(68.1)	1118	2.01(50.1)	8.84(49.9)	5.42
BA@DIN	557.16(30.7)	1662.53(69.3)	1324	2.23(56.5)	9.73(43.5)	5.49
BA@IMI	467.39(25.3)	1632.87(74.7)	1338	2.00(52.4)	11.13(47.6)	6.35

Table S7. Emission lifetimes ($\tau_{1\text{-}2,\ s}$) and fractions of the emission intensity ($f_{1\text{-}2}$, %) obtained from the fitting of experimental emission decay data by two-exponential functions of different materials, recorded at different detection temperatures, from which the average emission lifetimes τ_{avg} were calculated.

Sample	Temperature (k)	τ_1 (f_1)	τ_2 (f_2)	$\tau_{avg\ (s)}$
BA@THM	77K	0.28(47.1)	1.26(52.9)	0.80
	298K	0.37(67.4)	0.13(32.6)	0.29
BA@NIT	77K	0.18(11.4)	1.11(88.6)	1.01
	298K	0.06(5.1)	0.90(94.9)	0.86
BA@ACE	77K	0.03(6.0)	1.29(94.0)	1.21
	298K	0.01(35.6)	0.23(64.4)	0.15
BA@DIN	77K	0.62(28.0)	1.98(72.0)	1.59
	298K	0.18(21.6)	0.96(78.4)	0.79
BA@IMI	77K	1.75(82.4)	0.45(17.6)	1.52

	298K	0.52(92.3)	0.02(7.7)	0.48

Table S8. The energy gap between the singlet state and triplet states of pure NNI and corresponding host-guest materials.

Sample	ΔE_{st} (eV)	Sample	ΔE_{st} (eV)
THM	0.50	BA@THM	0.84
NIT	0.03	BA@NIT	0.80
ACE	-0.08	BA@ACE	0.62
DIN	0.34	BA@DIN	0.43
IMI	0.33	BA@IMI	0.58

Table S9. Detection performances of the assay for different types of NNI.

Analytes	Linear range ($\mu g \cdot mL^{-1}$)	LOD ($\mu g \cdot mL^{-1}$)
THM	4.20-76.91	0.02
NIT	0.13-5.13	0.04
ACE	0.62-31.15	0.02
DIN	1.49-45.51	0.02
IMI	1.01-23.47	0.01

Table S10. Comparison of the detection performance of our assay with recently reported works.

Detection method	Analyte	LOD (μg / L)	Linear range (μg / L)	Ref
QB - ICA	IMI	14.58	10-240	Sensors & Actuators: B. Chemica l361 (2022) 131671

	THM	0.36	0.5-10	
Fluorescence sensor	THM	0.36	2.92 ~ 2917.1	Analyst 146 (2021) 1986
	THM	0.08	0.3-50.0	
HPLC / DAD	IMI	0.08	0.3-50.0	Food Chemistry 367 (2022) 130653
	ACE	0.08	0.3-50.0	
MCH/Apt/AuNPs/ rGO/SPE	THM	0.00836	0.01 ~ 100	Microchemical Journal 207 (2024) 112169
	IMI	1.4		
OBP_2- DiNM	ACE	1.5	-	Biosensors and Bioelectronics 239 (2023) 115630
	DIN	4.5		
Co_3O_4@g-C_3N_4/ SPCE	THM	1.43	2.92 ~ 122518.2	Ecotoxicology And Environmental Safety189 (2020) 110035
QDs-SA-FLISA	IMI	0.5	0.50-5.72	Talanta 275 (2024) 126128
ic-ELISA		-	2.85-54.34	
GO/GCE	THM	2421.19	2917.1 ~ 58342	Biosensors and Bioelectronics 89 (2017) 532
GO- $CoFe_2O_4$@SiO_2-MIL101(Cr)-NH_2- UA-MSPE	ACE	0.022	0.074–3500	Talanta 217 (2020) 121120
	IMI	0.019	0.064–3500	

Table S11. Types and concentrations of interference species.

Interference Species		(μg / g)
Inorganic Anion	F^-	230
	PO_4^{3-}	1200
	SO_4^{2-}	760
	Cl^-	710
	NO_2^-	120
Amino Acid	Arg	2200
	Glu	7800
	Ala	600
	Thr	1000
	Lys	600
	His	400
Metal Ions	K^+	10200
	Ca^{2+}	2750
	Fe^{3+}	390
	Zn^{2+}	40
Organic Acid	OA	525.34
	AcOH	1.12

	α-KG	0.0132
	H_2MA	283.56
	CA	537.28
	FA	50.4
	SA	0.02
SMX	SD	0.2
	AZ	0.14
	CHL	0.076
Pesticides	TEB	0.13
	PM	0.872
	BOS	0.336

Table S12. Emission lifetimes ($\tau_{1\text{-}2,\ ms}$) and fractions of the emission intensity ($f_{1\text{-}2}$, %) obtained from the fitting of experimental emission decay data by two-exponential functions of different materials, recorded at different mixed ratios, from which the average emission lifetimes τ_{avg} were calculated.

Sample	**Ratios**	**τ_1 (f_1)**	**τ_2 (f_2)**	**$\tau_{avg\ (ms)}$**
	0%:100%	248.92(32.1)	1079.00(67.9)	812.54
NIT:ACE	25%:75%	309.24(22.6)	1001.22(77.4)	844.90
	50%:50%	334.39(22.9)	1017.60(77.1)	861.22

	75%:25%	341.41(20.0)	1006.48(80.0)	873.27
	100%:0%	345.47(22.4)	1075.21(77.6)	911.89
	0%:100%	293.69(47.4)	1095.92(52.6)	715.50
	25%:75%	355.03(27.2)	1257.83(72.8)	1012.09
NIT:DIN	50%:50%	368.45(25.4)	1192.24(74.6)	982.84
	75%:25%	396.76(25.4)	1137.66(74.6)	949.77
	100%:0%	345.47(2204)	1075.21(77.6)	911.89
	0%:100%	293.69(47.4)	1095.92(52.6)	715.50
	25%:75%	325.96(43.2)	1425.97(56.8)	950.33
ACE:DIN	50%:50%	360.29(38.4)	1583.69(61.6)	1113.66
	75%:25%	344.79(33.0)	1539.79(67.0)	1145.32
	100%:0%	248.92(32.1)	1079.00(67.9)	812.54

Table S13. Emission lifetimes ($\tau_{1\text{-}2,\ ms}$) and fractions of the emission intensity ($f_{1\text{-}2}$, %) obtained from the fitting of experimental emission decay data by two-exponential functions of different materials, recorded at different mixed ratios, from which the average emission lifetimes τ_{avg} were calculated.

Sample	**Ratios**	**τ_1 (f_1)**	**τ_2 (f_2)**	**τ_{avg}**
	0%:0%:100%	293.69(47.4)	1095.92(52.6)	715.50
NIT:ACE:DIN	100%:0%:0%	345.47(22.4)	1075.21(77.6)	911.89
	0%:100%:0%	248.92(32.1)	1079.00(67.9)	812.54

	25%:50%:25%	656.56(38.3)	1783.60(61.7)	1351.95
	50%:25%:25%	606.26(41.4)	1560.42(58.6)	1165.21
	25%:25%:50%	612.63(31.5)	1710.48(68.5)	1364.21